Applied Surface Science 254 (2008) 6455–6460

Contents lists available at ScienceDirect

Applied Surface Science

journal homepage: www.elsevier.com/locate/apsusc

Optical inhomogeneity of ZnS films deposited by thermal evaporation

Xiaochun Wu, Fachun Lai *, Limei Lin, Jing Lv, Binping Zhuang, Qu Yan, Zhigao Huang

School of Physics and Opto-Electronics Technology, Fujian Normal University, Shangsan Load, Cangshan Borough, Fuzhou 350007, PR China

ARTICLE INFO

Article history:
Received 22 February 2008
Received in revised form 31 March 2008
Accepted 1 April 2008
Available online 15 April 2008

Keywords:
ZnS
Thin films
Optical properties
Optical inhomogeneity

ABSTRACT

Zinc sulfide (ZnS) films with optical thickness (reference wavelength is 620 nm) ranging from 310 to 1240 nm were deposited on quartz substrates at room temperature by a thermal evaporation system. The structure and morphology of the films were investigated by X-ray diffraction, atomic force microscopy, respectively. The optical properties of the films were determined by in situ transmittance measurements and wideband spectra photometric measurements, respectively. The experimental results show that the films exhibit cubic structure, and the intensity of the (2 2 0) diffraction peak enhances with the increase of optical thickness. Surface grain size and surface roughness increase monotonously with increasing film thickness. Refractive indices and extinction coefficients calculated by in situ transmittance measurements are well consistent with those calculated by wideband spectra photometric measurements. Both the refractive index and packing density of the film increase as the increase of film thickness, which confirms the film is positive inhomogeneous and has an expanding columnar structure. Extinction coefficients of the films increase with increasing film thickness, which results from the increase of surface roughness.

© 2008 Elsevier B.V. All rights reserved.

www.spm.com.cn

1. Introduction

Zinc sulfide (ZnS), with a wide direct optical gap of 3.7 eV, has unique physical properties, such as high refractive index, low optical absorption in the visible and infrared spectral region. ZnS films, therefore, are widely used in many optical and electronic areas. II–VI compounds semiconductors are well known for applications in a wide range of optoelectronic devices, electro-optics modulator, optical coating, heterojunction solar cells. Generally CdS and CdTe are the most extensively used materials as a buffer layer in solar cells [1]. However, due to the toxic hazards with respect to the production and use of CdS layers, much attention has been focused on developing Cd-free buffer layers. One such possible replacement of CdS is ZnS [2].

Many deposition techniques have been used to prepare ZnS thin films, such as sputtering [3], pulsed-laser deposition [4,5], chemical vapor deposition [6–8], electron beam evaporation [9], thermal evaporation [10], photochemical deposition [11], pulsed electrochemical deposition [12] and chemical bath deposition [13]. Among these methods, thermal evaporation is the most common method in producing thin film because the advantages of thermal evaporation are stability, reproducibility, and high-deposition rate. It is well known that the optical parameters of thin-film materials are generally different from those of the same materials in bulk form. The differences in optical parameters depend very much on the conditions in which the deposition has been carried out. Previously, there were a lot of reports on the inhomogeneity of refractive index in thin films [14–21]. Khawaja et al. [14] studied the optical inhomogeneity of CeO_2 films deposited by electron beam evaporation. Optical inhomogeneity and microstructure of ZrO_2 films prepared by Ar-ion-assisted electron beam evaporation were investigated by Cho and Hwangbo [19]. Lai et al. [20] used a simple two-step film envelope method to determine the optical constants and small inhomogeneity of Nb_2O_5–TiO_2 mixed films. ZnS films have been applied in various modern technologies. However, few investigations on the inhomogeneity of ZnS films have been reported [21]. In present study, we focus on the optical inhomogeneity of ZnS films prepared by thermal evaporation. Refractive indices and extinction coefficients of the films with different optical thicknesses were calculated by in situ transmittance measurements and wideband spectra photometric measurements, respectively. Additionally, the crystal structure, surface morphology and packing density of the films were investigated.

2. Determination of optical constants by in situ transmittance measurements

A lot of approaches have been used to determine the refractive index (n) and extinction coefficient (k) of a thin film. In present study, the envelope method proposed by Swanepoel [22] was

* Corresponding author. Tel: +86 591 22868137; fax: +86 591 22868132.
E-mail address: laifc@fjnu.edu.cn (F. Lai).

0169-4332/$ – see front matter © 2008 Elsevier B.V. All rights reserved.
doi:10.1016/j.apsusc.2008.04.023

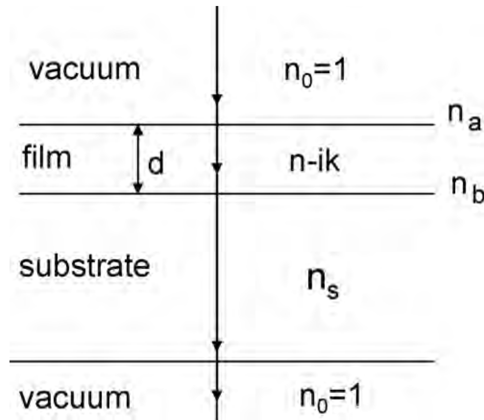

Fig. 1. Schematic illustration of a thin weakly absorbing inhomogeneous film on a thick finite transparent substrate.

applied to the determination of optical parameters from transmittance spectra. Fig. 1 is the schematic illustration of a thin weakly absorbing inhomogeneous film deposited on a thick finite transparent substrate. Supposing the film has thickness d and complex refractive index $n - ik$. n_a and n_b are the refractive indices of the film at the vacuum side and substrate side, respectively. Thickness of the substrate is several orders of magnitude larger than d, which means that the optical interference effect of the substrate can be neglected. Refractive index of the substrate (n_s) assumed to be known. The expression for the transmittance of a weakly absorbing inhomogeneous film on a transparent substrate at normal incidence can be given by [18]

$$T = \frac{Ax}{B - Cx\cos\theta + Dx^2} \quad (1)$$

where

$$A = 16n_0^2 n_a n_b n_s$$
$$B = (n_a + n_0)^2 (n_b + n_0)(n_0 n_b + n_s^2)$$
$$C = 2n_0 (n_a^2 - n_0^2)(n_b^2 - n_s^2)$$
$$D = (n_a - n_0)^2 (n_b - n_0)(n_0 n_b - n_s^2)$$
$$\theta = \frac{4\pi \bar{n} d}{\lambda}, \qquad x = \exp(-\alpha d), \quad \alpha = \frac{4\pi \bar{k}}{\lambda}$$

$\bar{n}$ and $\bar{k}$ are the average refractive index and extinction coefficient, respectively. $\bar{n}$ and $\bar{k}$ can be expressed by

$$\bar{n} = \frac{1}{nd}\int_0^{nd} n(nd)\,\mathrm{d}(nd) \quad (2)$$

$$\bar{k} = \frac{1}{nd}\int_0^{nd} k(nd)\,\mathrm{d}(nd) \quad (3)$$

For $n_b > n_s$, at the quarter-wave points where the optical thickness of the film is a multiple of the quarter-wave length, the extrema of the transmittance can be written as

$$T_M = \frac{Ax}{B - Cx + Dx^2} \quad (4)$$

$$T_m = \frac{Ax}{B + Cx + Dx^2} \quad (5)$$

Where T_M is the maxima and T_m is the minima. In the following calculation, both T_M and T_m are the correspondence in the identical optical thickness, which can be gained by the envelopes of the extrema.

Substituting Eq. (4) into Eq. (5) yields

$$\left(\frac{1}{T_m} - \frac{1}{T_M}\right) = \frac{2C}{A} = \frac{(n_a^2 - 1)(n_b^2 - n_s^2)}{4n_s n_a n_b} \quad (6)$$

In order to get the innermost refractive index, we let $n_a = n_b$, solving Eq. (6) gives

$$n_b = \left[N + \sqrt{N^2 - n_s^2}\right]^{1/2} \quad (7)$$

where

$$N = 2n_s \frac{T_M - T_m}{T_M T_m} + \frac{1}{2}(n_s^2 + 1)$$

The other refractive indices at the quarter-wave points can be given

$$n_a = \frac{M + \sqrt{M^2 + 4}}{2} \quad (8)$$

where

$$M = \frac{4n_s n_b((T_M - T_m)/T_M T_m)}{n_b^2 - n_s^2}$$

Adding the reciprocals of Eqs. (4) and (5) yields

$$\frac{1}{T_m} + \frac{1}{T_M} = 2\frac{Dx^2 + B}{Ax} \quad (9)$$

Solving for x gives

$$x = \frac{A(T_M + T_m)/T_M T_m - \sqrt{(A(T_M + T_m)/T_M T_m)^2 - 16DB}}{4D} \quad (10)$$

So the extinction coefficient at the quarter-wave points can be calculated by

$$x = \exp\left(-\frac{4\pi k d}{\lambda}\right) \quad (11)$$

3. Experimental details

ZnS films with different optical thicknesses of 310, 620, 930, 1240 nm were deposited by thermal evaporation technique. The quartz substrates of 2.5-cm diameter were cleaned in acetone and ethanol before deposition. The base vacuum level was 3.0×10^{-3} Pa, and the deposition pressure was about 5.0×10^{-3} Pa. The substrates were placed in a sample holder and kept at a distance of 30 cm from the evaporation source. The substrate holder was connected to an electric motor to rotate the substrate during the deposition to achieve uniform film. Electric current for evaporation was 130 A. The nominal film thickness was controlled by an optical thickness monitor. The reference wavelength of optical monitor was 620 nm. In order to obtain the refractive index, extinction coefficient and their variation as the increase of film thickness, the transmittance at the quarter-wave points was recorded by in situ transmittance measurements.

The crystal structure of ZnS films was examined by X-ray diffraction (XRD). XRD study was carried out on an X-ray diffractometer (RIGAKU D/MAX2500) with high-intensity Cu Kα radiation (λ = 1.5418 Å). The surface morphology of ZnS films was observed with an atomic force microscopy (AFM) (CSPM 400) under ambient conditions. The root mean square (RMS) surface roughness of the films was calculated from AFM images. Scans with a resolution of 512 × 512 pixels, were taken under a contact force of 10^{-9} N and over areas of 4 μm × 4 μm for calculation of RMS surface roughness. The normal incidence transmittance of the films was investigated with a double-beam spectrophotometer (UV-2450) in

www.spm.com.cn

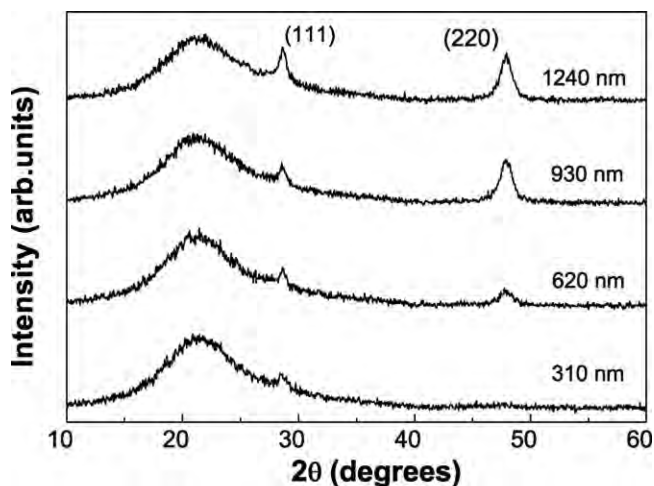

Fig. 2. X-ray diffraction patterns for ZnS films with different optical thicknesses.

the wavelength range 300–900 nm. Refractive indices and extinction coefficients of the films with different optical thicknesses were also determined from all transmittance data [23].

4. Results and discussion

4.1. Crystal structure

Fig. 2 shows the XRD patterns of ZnS films with different optical thicknesses. Comparing the diffraction peaks position with the data from JCPDS international diffraction data base, it is found that the peaks at 28.7° and 48.0° correspond to (1 1 1) and (2 2 0) planes of ZnS, respectively with cubic structure [24]. As shown in Fig. 2, the XRD pattern of the film with 310-nm optical thickness shows only (1 1 1) peak. However, for sample with 620-nm optical thickness, a new (2 2 0) peak appears in the XRD pattern. Additionally, the intensity of both (1 1 1) and (2 2 0) peaks enhances monotonously with increasing film thickness. As the optical thickness of the films increases to 1240 nm, the intensity of (2 2 0) peak is stronger than that of (1 1 1) peak. This change in film structure is due to the increase of the substrate temperature and film thickness [18,25].

4.2. Surface morphology

AFM images with 4 μm × 4 μm areas of the films with different optical thicknesses are shown in Fig. 3. As indicated in Fig. 3, all films show smooth surface morphology. RMS surface roughness and average surface grain size were calculated from AFM images. The average surface grain size increases from 24.2 to 31.4 nm as the optical thickness increases from 310 to 1240 nm. Accordingly, RMS surface roughness increases gradually from 1.16 to 4.22 nm. The increase of surface roughness and surface grain size with increasing film thickness attributes to the improvement of the crystallinity of the films as discussed in XRD result.

4.3. Optical properties

4.3.1. Method of in situ transmittance measurements

Table 1 lists the extrema of transmittance at the quarter-wave points, which recorded by in situ transmittance measurements,

www.spm.com.cn

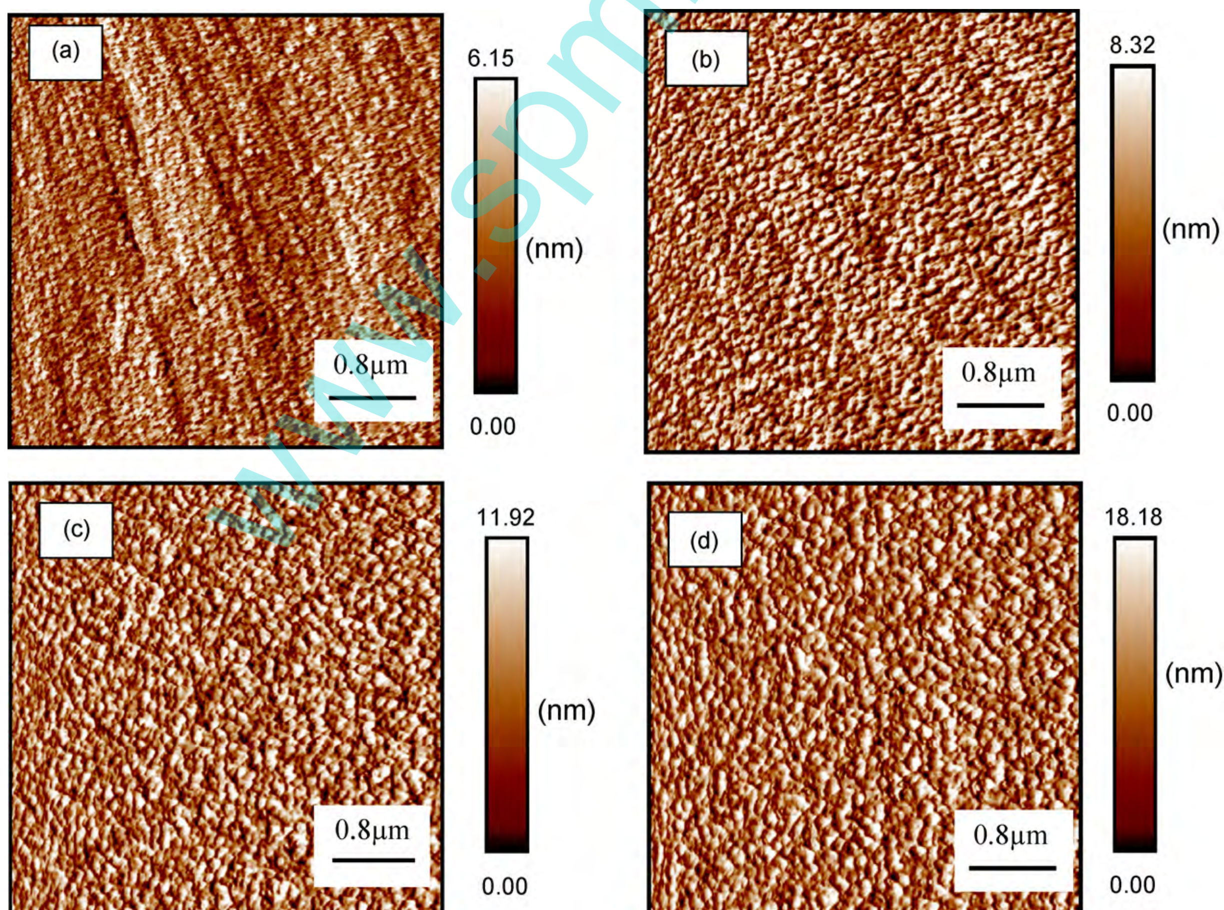

Fig. 3. AFM images of the ZnS films with different optical thicknesses: (a) 310 nm, (b) 620 nm, (c) 930 nm and (d) 1240 nm.

Table 1
Transmittance at the quarter-wave points recorded by in situ transmittance measurements

Optical thickness (nm)	Transmittance
0	0.933
155	0.654
310	0.892
465	0.630
620	0.853
775	0.602
930	0.802
1085	0.581
1240	0.786

and the total optical thickness of ZnS film is 1240 nm. The monitoring wavelength was 620 nm and the substrates were not heated. As can be seen in Table 1, the values of the maxima and minima of the transmittance decrease with increasing film thickness. The maxima decrease from 0.933 to 0.786, and the minima decrease from 0.654 to 0.581. Using the data in Table 1 and Eqs. (7)–(11), refractive index and extinction coefficient of the film can be calculated. Variations of n and k as the increase of film thickness are shown in Figs. 4 and 5, respectively. As shown in Fig. 4, the solid squares show the refractive indices at the quarter-wave optical thicknesses and the solid line is the refractive indices curve fitting by a parabolic interpolation. n of ZnS film increases with thickness in the direction of film growth (positive inhomogeneity), which indicates that the columnar structure of the film is an expanding columns with a packing density of larger than 0.9069 [21]. This result indicates that the void fraction of the top layer next to air is smaller than that of the bottom one. As indicated in Fig. 5, k of the film increases from about 0.78×10^{-3} to 1.15×10^{-3} as optical thickness increases from 150 to 1200 nm. The increase of surface roughness (Fig. 3) with increasing film thickness for crystalline film will increase surface optical scattering and optical loss [25,26], which induces the increase of extinction coefficient.

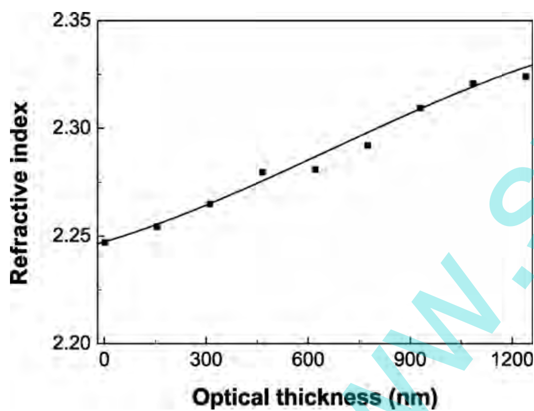

Fig. 4. Variation of refractive index as a function of the optical thickness determined by in situ transmittance measurements. The reference wavelength is 620 nm.

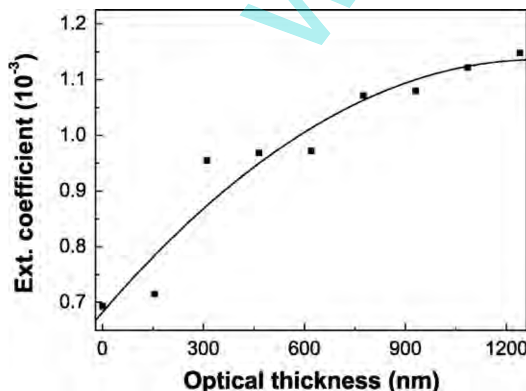

Fig. 5. Variation of extinction coefficient at different optical thicknesses calculated by in situ transmittance measurements. The reference wavelength is 620 nm.

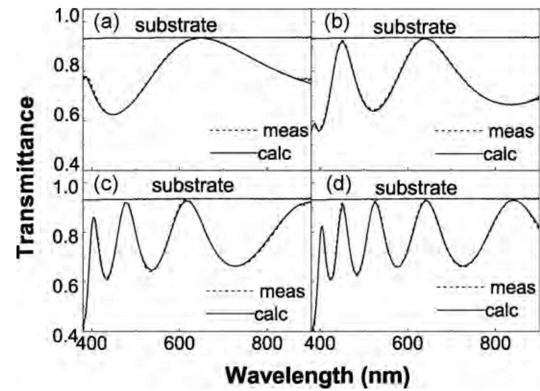

Fig. 6. Measured (dash line) and calculated (solid line) transmittance for ZnS films with different optical thicknesses: (a) 310 nm, (b) 620 nm, (c) 930 nm and (d) 1240 nm.

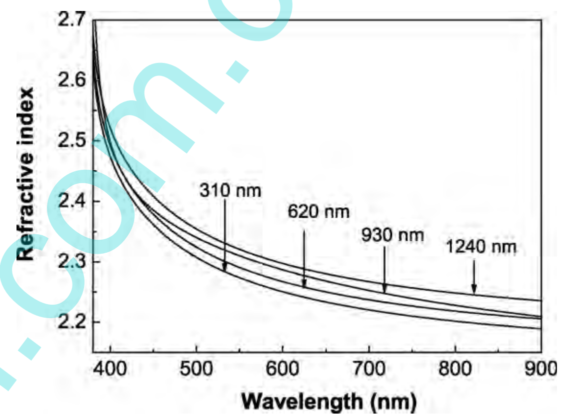

Fig. 7. Average refractive index curves of ZnS films with different optical thicknesses.

4.3.2. Method of wideband spectra photometric measurements

The transmittance with optical wavelength from 300 to 900 nm of ZnS films with optical thickness of 310, 620, 930 and 1240 nm was measured by a spectrophotometer, and the result is shown in

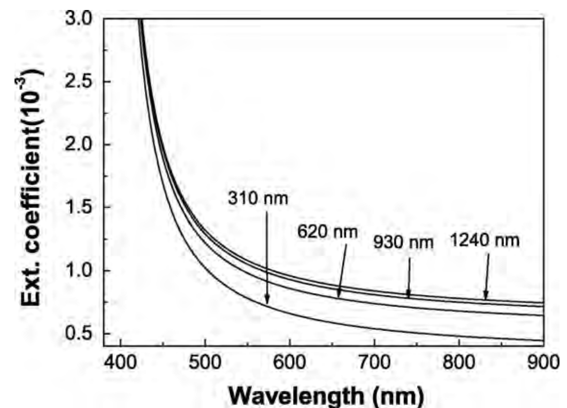

Fig. 8. Average extinction coefficients as a function of wavelength for ZnS films with different optical thicknesses.

www.spm.com.cn

Table 2
Average refractive indices ($\bar{n}$) and extinction coefficients ($\bar{k}$) of the films with different optical thicknesses calculated by in situ transmittance measurements and wideband spectra photometric measurements

Optical thickness (nm)		310	620	930	1240
In situ transmittance measurements	$\bar{n}$	2.252 ± 0.007	2.263 ± 0.012	2.278 ± 0.018	2.287 ± 0.025
	$\bar{k}(10^{-4})$	7.8 ± 0.6	8.7 ± 0.9	9.4 ± 1.2	10.1 ± 1.4
Wideband spectra photometric measurements	$\bar{n}$	2.243 ± 0.008	2.261 ± 0.015	2.280 ± 0.021	2.289 ± 0.024
	$\bar{k}(10^{-4})$	6.3 ± 0.5	8.3 ± 0.9	9.0 ± 1.1	9.2 ± 1.3

The reference wavelength is 620 nm.

Fig. 6. The average refractive indices ($\bar{n}$) and extinction coefficients ($\bar{k}$) of these films were retrieved from all the normal incidence transmittance data (in Fig. 6) [23], and the results are presented in Figs. 7 and 8. As shown in Fig. 6, the calculated transmittances are in good agreement with the measured data in the overall measured wavelength range, which confirms the reliability of $\bar{n}$ and $\bar{k}$. As can be seen in Fig. 7, $\bar{n}$ increases gradually as the film thickness increases. Additionally, $\bar{k}$ also increases with the increase of film thickness as shown in Fig. 8. n and k increase with increasing film thickness is well consistent with the results determined by in situ transmittance measurements.

Based on the data in Fig. 4 and Eqs. (1)–(3), $\bar{n}$ and $\bar{k}$ of the films can be determined from in situ transmittance measurements, too. Table 2 lists $\bar{n}$ and $\bar{k}$ calculated from in situ transmittance measurements and wideband spectra photometric measurements, respectively, and the reference wavelength is 620 nm. In addition, standard deviations of $\bar{n}$ and $\bar{k}$ are also listed in Table 2. As can be seen in Table 2, $\bar{n}$ calculated by wideband spectra photometric measurements is in good agreement with that calculated by in situ transmittance measurements. However, $\bar{k}$ calculated by wideband spectra photometric measurements is less than that calculated by in situ transmittance measurements, which is the result of the different formulas for calculation of $\bar{k}$ [18]. $\bar{k}$ determined from in situ transmittance measurements is based on the extrema of the transmittance, which results in a little increase of the calculated $\bar{k}$ [20]. Standard deviations for both $\bar{n}$ and $\bar{k}$, as shown in Table 2, increase with increasing film thickness, which is the result of the increase of n and k as the increase of film thickness.

In order to study the relationship between optical inhomogeneity and film columnar structure, a relationship between n and packing density (p) based on Lorentz–Lorenz polarization theory has been educed by Harris et al. [21]. The packing density of ZnS film can be determined by

$$p = \frac{(n_c^2 + 2)(n^2 - n_v^2)}{(n_c^2 - n_v^2)(2 + n^2)} \quad (12)$$

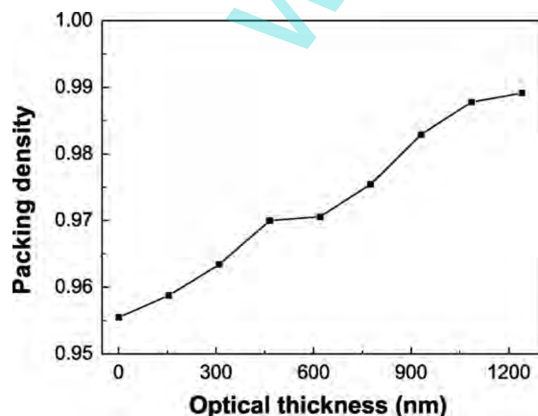

Fig. 9. Variation of the packing density of ZnS film as a function of optical thickness.

where n_c and n_v are the refractive indices of the columnar solid ($n_c = 2.35$) for ZnS [21] and air surrounding voids ($n_v = 1$), respectively. Using Eq. (12) and n at the quarter-wave points (in Fig. 4) determined from in situ transmittance measurements, p of ZnS film was calculated and the results are shown in Fig. 9. As presented in Fig. 9, p increases from 0.96 to 0.99 when the optical thickness increases from 155 to 1240 nm. The increase of p with increasing film thickness is the result of the expanding columnar structure of the film.

5. Conclusion

ZnS films with different optical thicknesses were deposited by a thermal evaporation system at room temperature. The optical inhomogeneity of the films was investigated by in situ transmittance measurements and wideband spectra photometric measurements, respectively. The refractive indices determined by the method of in situ transmittance measurements are in good agreement with those determined by the method of wideband spectra photometric measurements. The experimental results show that the refractive index, extinction coefficient and packing density increase with increasing film thickness. The films are positive inhomogeneity and have an expanding columnar structure. XRD results show that the crystallinity of the film improves as the film thickness increases. AFM results indicate that surface roughness and surface grain size increase with increasing film thickness, which results in the increase of extinction coefficient.

Acknowledgments

This work was financially supported by Natural Science Foundation of Fujian Province of China (2007J0317) and Key project of Fujian Provincial Department of Science and Technology (2007H0019).

References

[1] T. Wada, Y. Hashimoto, S. Nishiwaki, T. Satoh, S. Hayashi, T. Negami, H. Miyake, Solar Energy Mater. Solar Cells 67 (2001) 305.
[2] B. Asenjo, A.M. Chaparro, M.T. Gutiérrez, J. Herrero, J. Klaer, Solar Energy Mater. Solar Cells 92 (2008) 302.
[3] A. Nitta, K. Tanaka, Y. Maekawa, M. Kusabiraki, M. Aozasa, Thin Solid Films 384 (2001) 261.
[4] K.T. Hillie, H.C. Swart, Appl. Surf. Sci. 253 (2007) 8513.
[5] S. Yano, R. Schroeder, H. Sakai, B. Ullrich, Appl. Phys. Lett. 82 (2003) 2026.
[6] Q.J. Feng, D.Z. Shen, J.Y. Zhang, H.W. Liang, D.X. Zhao, Y.M. Lu, X.W. Fan, J. Crystal Growth 285 (2005) 561.
[7] Z.Z. Zhang, D.Z. Shen, J.Y. Zhang, C.X. Shan, Y.M. Lu, Y.C. Liu, B.H. Li, D.X. Zhao, B. Yao, X.W. Fan, Thin Solid Films 513 (2006) 114.
[8] Y. Drezner, S. Berger, M. Hefetz, Mater. Sci. Eng. B 87 (2001) 59.
[9] S. Wang, X. Fu, G. Xia, J. Wang, J. Shao, Z. Fan, Appl. Surf. Sci. 252 (2006) 8734.
[10] P. Prathap, Y.P.V. Subbaiah, K.T.R. Reddy, R.W. Miles, J. Phys. D: Appl. Phys. 40 (2007) 5275.
[11] M. Gunasekaran, R. Gopalakrishnan, P. Ramasamy, Mater. Lett. 58 (2003) 67.
[12] N. Fathy, R. Kobayashi, M. Ichimura, Mater. Sci. Eng. B 107 (2004) 271.
[13] P. Roy, J.R. Ota, S.K. Srivastava, Thin Solid Films 515 (2006) 1912.
[14] E.E. Khawaja, S.M.A. Durrani, M.F. Al-Kuhaili, J. Phys. D: Appl. Phys. 36 (2003) 545.
[15] M. Montecchi, R.M. Montereali, E. Nichelatti, Thin Solid Films 396 (2001) 262.

www.spm.com.cn

[16] J.P. Borgogno, F. Flory, P. Roche, B. Schmitt, G. Albrand, E. Pelletier, H.A. Macleod, Appl. Opt. 23 (1984) 3567.
[17] A.V. Tikhonravov, M.K. Trubetskov, B.T. Sullivan, J.A. Dobrowolsk, Appl. Opt. 36 (1997) 7188.
[18] Y.Y. Liou, C.C. Lee, C.C. Jaing, C.W. Chu, J.C. Hsu, Jpn. J. Appl. Phys. 34 (1995) 1952.
[19] H.J. Cho, C.K. Hwangbo, Appl. Opt. 35 (1996) 5545.
[20] F. Lai, Y. Wang, M. Li, H. Wang, Y. Song, Y. Jiang, Thin Solid Films 515 (2007) 4763.
[21] M. Harris, H.A. Macleod, S. Ogura, Thin Solid Films 57 (1979) 173.
[22] R. Swanepoel, J. Phys. E: Sci. Instrum. 16 (1983) 1214.
[23] L. Lin, F. Lai, Z. Huang, Y. Qu, R. Gai, Proc. SPIE 6149 (2005), 614920.
[24] I.V. Dubrovin, L.D. Budennaya, I.B. Mizetskaya, E.V. Sharkina, Inorg. Mater. 19 (1983) 1603 (Reference No. 65-0309 in PCPDFWIN (Version 2.02). JCPDS-International Centre for Diffraction Data).
[25] F. Lai, L. Lin, Z. Huang, R. Gai, Y. Qu, Appl. Surf. Sci. 253 (2006) 1801.
[26] F. Lai, M. Li, H. Wang, H. Hu, X. Wang, J.G. Hou, Y. Song, Y. Jiang, Thin Solid Films 488 (2005) 314.

www.spm.com.cn